

## Absolutely Stable Time Crystals at Finite Temperature

Francisco Machado<sup>1,2,3,4,\*</sup> Quntao Zhuang<sup>3,5,6,\*</sup> Norman Y. Yao<sup>2,3,4</sup> and Michael P. Zaletel<sup>3,4</sup>

<sup>1</sup>*ITAMP, Harvard-Smithsonian Center for Astrophysics, Cambridge, Massachusetts 02138, USA*


<sup>2</sup>*Department of Physics, Harvard University, Cambridge, Massachusetts 02138, USA*

<sup>3</sup>*Department of Physics, University of California, Berkeley, Berkeley, California 94720, USA*

<sup>4</sup>*Materials Science Division, Lawrence Berkeley National Laboratory, Berkeley, California 94720, USA*

<sup>5</sup>*James C. Wyant College of Optical Sciences, University of Arizona, Tucson, Arizona 85721, USA*

<sup>6</sup>*Ming Hsieh Department of Electrical and Computer Engineering and Department of Physics and Astronomy, University of Southern California, Los Angeles, California 90089, USA*

 (Received 22 October 2022; revised 27 July 2023; accepted 7 September 2023; published 1 November 2023)

We show that locally interacting, periodically driven (Floquet) Hamiltonian dynamics coupled to a Langevin bath support finite-temperature discrete time crystals (DTCs) with an infinite autocorrelation time. By contrast to both prethermal and many-body localized DTCs, the time crystalline order we uncover is stable to arbitrary perturbations, including those that break the time translation symmetry of the underlying drive. Our approach utilizes a general mapping from probabilistic cellular automata to open classical Floquet systems undergoing continuous-time Langevin dynamics. Applying this mapping to a variant of the Toom cellular automaton, which we dub the “ $\pi$ -Toom time crystal,” leads to a 2D Floquet Hamiltonian with a finite-temperature DTC phase transition. We provide numerical evidence for the existence of this transition, and analyze the statistics of the finite temperature fluctuations. Finally, we discuss how general results from the field of probabilistic cellular automata imply the existence of discrete time crystals (with an infinite autocorrelation time) in all dimensions,  $d \geq 1$ .

DOI: [10.1103/PhysRevLett.131.180402](https://doi.org/10.1103/PhysRevLett.131.180402)

A tremendous amount of recent excitement has centered upon interacting periodically driven (Floquet) “phases of matter” [1–7]. While discussed as nonequilibrium phases, thus far attention has largely focused on two scenarios which are nonequilibrium only in a rather restricted sense. First, there are quantum “many-body-localized” (MBL) Floquet phases [2–4,8–11]. Because the ergodicity breaking of MBL is sufficient to prevent the periodic drive from heating the system to infinite temperature, the system does not need to be coupled to a dissipative bath (e.g., the dynamics are driven, but purely unitary) [12–14]. In this case, the eigenstates of the Floquet evolution have area-law entanglement, which allows much of the physics to be mapped to more familiar questions of order in quantum ground states [15–18]. Second, there are “prethermal” Floquet phases, in both classical and quantum systems, which heat exponentially slowly due to (for example) a mismatch between the driving frequency and the natural frequencies of the undriven system [19–28]. During the exponentially long timescale before heating, these systems can exhibit behavior which is analogous to order in finite temperature equilibrium phases [20,24,26,27]. However, prethermal Floquet phases are not “true” phases in the strict sense because they are distinguished from disordered behavior via crossovers, rather than sharp transitions [7].

Perhaps the most paradigmatic example of a Floquet phase of matter is the so-called discrete time crystal

(DTC)—starting from a generic initial state, at long times the DTC relaxes into a steady state with a temporal periodicity which is a multiple of the drive’s [2–4]. This behavior breaks the discrete time-translation symmetry of the drive and is stable to small perturbations of the dynamics.

From the perspective of symmetry breaking, it is natural to ask if “true” time crystals, with an infinite autocorrelation time, exist beyond many-body localized quantum systems [29]; here, we emphasize that the lifetime of the DTC order should diverge exponentially in the system size as the thermodynamic limit is taken, while all other parameters (i.e., Floquet frequency, temperature, etc.) are kept fixed. Without an MBL phase to prevent heating, one requires an alternate strategy to stabilize time crystalline order; one approach that is compatible with both quantum and classical many-body dynamics is to couple the system to a dissipative bath [20,30–40].

Thinking microscopically, classical driven dissipative systems are described by Hamiltonian dynamics coupled to a finite-temperature Langevin bath, or in the quantum case, periodically driven Lindblad evolution. A key feature in both these contexts is that if the bath is dissipative, at finite temperature it should also come with noise due to the fluctuation-dissipation theorem. At zero temperature, where there is damping but no noise, many-body time crystals can occur rather trivially by analogy to the “period doubling” of coupled iterated logistic maps [41–45]. By contrast, the

presence of noise pushes the system to explore its entire phase space and can therefore desynchronize any initial time-crystalline behavior. This noise-induced ergodicity leads to a finite lifetime for the DTC order. The key question we will focus on is the following: Can true time crystals exist in a periodically driven system of locally interacting particles coupled to an equilibrium bath at finite temperature?

In this Letter, we argue in the affirmative: finite-temperature time crystals [46,47], with an *infinite* auto-correlation time, can exist even in translation-invariant arrays of classical nonlinear oscillators interacting only with their nearest neighbors. This significantly strengthens and extends upon prior works which found that arrays of parametrically driven oscillators did not produce a stable time crystal: thermal fluctuations led to an auto-correlation time which was finite and activated [48].

Our results are threefold. First, we explain [49] how nontrivial results in the field of probabilistic cellular automata (PCAs) [50,51] imply that local PCAs can exhibit time-crystalline behavior stable to arbitrary small perturbations in any dimension,  $d \geq 1$  [52–56]. Unlike MBL or prethermal time crystals, such time-crystalline order is “absolutely stable,” in the sense that it remains robust *even* in the presence of perturbations that break the discrete time-translation symmetry of the periodic drive. Next, we extend these PCA results to the physical setting of interest—classical, continuous-time, Langevin dynamics. In particular, we provide an explicit protocol which allows classical Langevin dynamics to “simulate” any PCA; focusing on the example of the so-called  $\pi$ -Toom PCA in 2D [54–56], we find that our continuous-time Langevin simulation indeed exhibits a finite-temperature phase transition between a discrete time crystal and a disordered phase (Fig. 1). Finally, we utilize results from “large deviations” theory to analytically obtain a bound on the spatiotemporal error cumulants; building on this bound, we perform an extensive analysis of the errors due to Langevin noise and provide numerical evidence that they are of a type covered by rigorous mathematical results from Gács and Toom [52–56].

*Time crystals in probabilistic cellular automata.*— Each state of a probabilistic cellular automata is given by a particular configuration  $\{\eta(\mathbf{x})\}$ , where  $\mathbf{x} \in \Lambda$  labels sites in a regular lattice  $\Lambda$  and each  $\eta(\mathbf{x})$  takes values in a finite set  $\mathcal{S}$ . In a conventional cellular automaton (CA), the dynamics are governed by a deterministic transition rule [79,80],

$$\{\eta(\mathbf{x}, t + 1)\} = \mathcal{T}\{\{\eta(\mathbf{x}, t)\}\}. \quad (1)$$

In a PCA, the dynamics are governed by a Markov process described by the transition matrix  $M_{\eta \rightarrow \eta'}$ , which characterizes the *probability* to evolve from configuration  $\eta$  to  $\eta'$  [81–83].

Whether a PCA can realize a stable time crystal is subtle. The long-time dynamics of a PCA are described by the

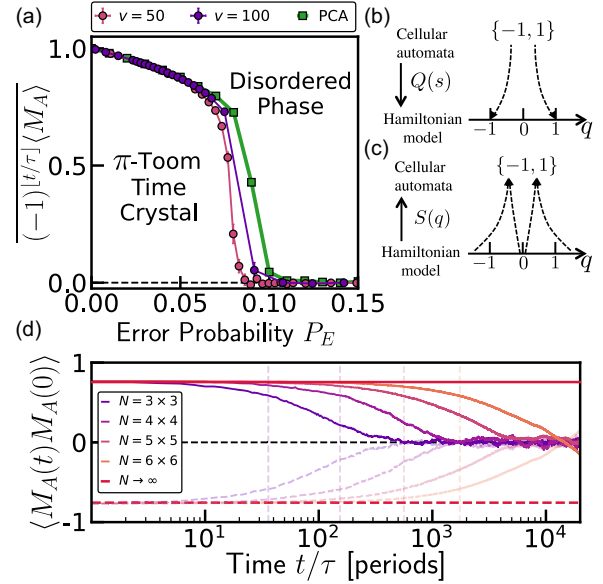


FIG. 1. (a) Time crystalline order parameter (e.g., stroboscopic magnetization) as a function of the error probability. The phase transition from a discrete time crystal to the disordered phase is shown for both a continuous-time, Floquet Langevin simulation of the  $\pi$ -Toom model with pinning potential  $v = 50, 100$ , as well as for a direct implementation of the  $\pi$ -Toom PCA. We average  $(-1)^{\lfloor t/\tau \rfloor} \langle M_A \rangle$  starting at  $t = 3000$  for  $\sim 500$  Floquet cycles,  $\sim 50$  noise realizations and system size  $N = 32 \times 32$ . (b),(c) Schematic of the translation between the discrete state space of a cellular automata and the continuous state space of a Hamiltonian model. (d) Dynamics of the Langevin  $\pi$ -Toom model ( $v = 100$ ,  $T = 7$ ), exhibiting robust period doubling (full line even times, light dashed line odd times) with a lifetime that grows exponentially with  $L$  [57]. We infer that for the system size ( $L = 32$ ) considered in panel (a), the lifetime of the  $\pi$ -Toom time crystal is significantly longer than the time window over which the magnetization is averaged.

stationary probability distributions  $\mathcal{P}[\eta]$  of  $M$ , e.g.,  $M\mathcal{P}[\eta] = \mathcal{P}[\eta]$ . We say  $M$  exhibits an  $n$ -fold subharmonic response if there are  $n > 1$  distinct distributions,  $\mathcal{P}_i[\eta]$ , such that  $M\mathcal{P}_i[\eta] = \mathcal{P}_{i+1}[\eta]$ , with  $\mathcal{P}_n = \mathcal{P}_0$ . This simply formalizes the notion of long-time oscillations: at long times, a generic initial state will relax into to a nonuniform convex combination  $\sum_i p_i \mathcal{P}_i$  which is stationary under  $M^n$ , but not  $M$  [84]. A PCA time crystal is then defined to be a local PCA with a *stable*  $n$ -fold subharmonic response. This motivates our first question: Do PCA time crystals exist [86]?

One prerequisite for a PCA time crystal is ergodicity breaking. A PCA is “ergodic” if it has a unique stationary distribution, so that at long times the state is independent of the initial spin configuration. A time crystal necessarily breaks ergodicity because  $M^n$  has  $n$  stationary distributions, so the system remembers which of the  $n$  states in the orbit it is in. Ergodicity-breaking PCAs were first proved to exist in 2D by Toom [54,81], and much later in 1D by Gács [52]. We focus our discussions here on Toom’s model because of

its simplicity (a discussion of the Gács model in 1D is provided in the Supplemental Material [57]). The Toom model is a 2D PCA with a binary state space,  $\mathcal{S} = \{-1, 1\}$ , and a “majority vote” transition rule in the northern-east-center (NEC) neighborhood  $\mathcal{N} = \{(1, 0), (0, 1), (0, 0)\}$  [each  $(\Delta x_i, \Delta y_i) \in \mathcal{N}$  denotes the relative locations of the cells in the neighborhood].

Crucially, in this model, it was proven that there are two “phases” (i.e., stationary distributions), corresponding to states “all +1” and “all -1,” which are stable against arbitrary stochastic perturbations below a critical error rate  $\epsilon$  [87], provided that the errors are not too correlated [52,54,88]. This requirement can be encoded into an error condition: there exists  $\epsilon$  such that the probability of  $k$  errors is bounded

$$P_{\wedge_{\ell=1}^k E_{u_\ell}} = \prod_{\ell=1}^k P_{E_{u_\ell} | E_{u_{\ell-1}}, \dots, E_{u_1}} \leq \epsilon^k, \quad (2)$$

where  $E_u$  denotes an “error” at a space-time point  $u$ , i.e., the dynamics did not follow the original update rule  $\mathcal{T}$ .

Finally, a simple modification of the Toom PCA [49,89], which we call the “ $\pi$ -Toom” model, immediately turns this construction into a time crystal exhibiting an infinite autocorrelation time [90]: in particular, instead of an NEC majority vote, one utilizes an NEC antimajority vote, or equivalently, one considers the Toom model with an interleaved spin flip,  $1 \leftrightarrow -1$ , between each step. In 1D, an equivalent construction based upon the Gács model yields a similar PCA time crystal.

*Simulating a PCA using Floquet-Langevin dynamics.*— In order to extend PCA time crystals to a microscopic, physical setting, we now demonstrate the ability for continuous-time Langevin dynamics to effectively simulate any PCA. The dynamics we consider take the general Langevin form

$$\begin{aligned} \dot{q}_i &= \partial_{p_i} H(\{p, q\}; t) \\ \dot{p}_i &= -\partial_{q_i} H(\{p, q\}; t) + R_i(t) - \gamma p_i \\ \langle R_i(t) R_j(t') \rangle_{\text{noise}} &= 2\gamma T \delta_{ij} \delta(t - t'), \end{aligned} \quad (3)$$

where  $(q_i, p_i)$  are the conjugate variables of a classical oscillator at site  $i$ , and  $R_i(t)$  is a stochastic force whose variance is proportional to the friction coefficient  $\gamma$  and the temperature  $T$ . We focus on a CA with states  $\eta \in \{-1, 1\}$  which we will encode in the oscillator with the identification  $\eta = \text{sign}(q)$  as depicted in Figs. 1(b) and 1(c).

The Hamiltonian takes the form  $H(t) = \sum_i (p_i^2/2m) + U(\{q\}, t)$ , with  $U(t)$  engineered so that one Floquet cycle,  $H(t + \tau) = H(t)$ , will implement one application of the update rule  $\mathcal{T}$ .

When attempting to build Floquet-Langevin dynamics that simulate a PCA, we encounter the following challenge. In our continuous-time dynamics, one needs a way to

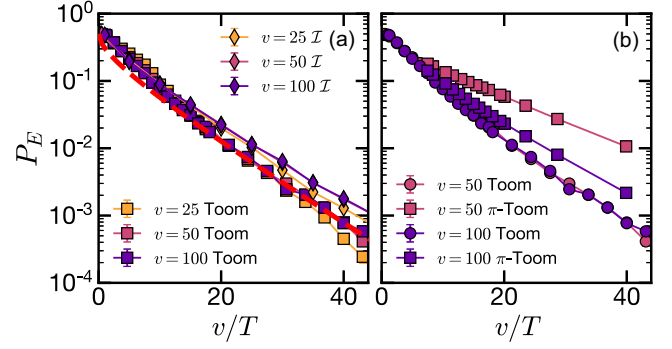


FIG. 2. Error probability  $P_E$  versus the ratio of the pinning potential to the temperature,  $v/T$ , in simulations of (a) the do-nothing ( $\mathcal{I}$ ) and Toom CAs. The dashed-red line indicates the equilibrium estimate  $P_E = \frac{1}{2} \text{erfc}(\sqrt{v_I/(2T)})$ . (b) The  $\pi$ -Toom CA. While  $P_E$  apparently depends on the simulated CA, as  $v$  increases the  $\pi$ -Toom error rate converges toward the Toom error rate. In all cases, we find an exponential decay in the error rate as a function of  $v/T$ . Data are obtained from a  $32 \times 32$  system by averaging over 25 Floquet cycles after an initial evolution of 200 Floquet cycles.

“store” the previous global state throughout the update cycle. This is essential in order to give the dynamics enough time to identify what the new state of the system should be. To solve this issue, at each position  $\mathbf{x}$ , we envision *two* oscillators ( $A$  and  $B$ ) with coordinates  $(q_x^A, p_x^A)$  and  $(q_x^B, p_x^B)$ . At each step, we will view one set of oscillators (say  $A$ ) as the “memory,” while the other set ( $B$ ) will undergo evolution to the new state  $B = \mathcal{T}(A)$ , driven by  $U(\{q\}, t) = V_I(\{q\})$ . After letting the particles relax to their positions using a pinning potential  $U(\{q\}, t) = \sum_i V_{\text{pin}}(q_i)$ , we exchange the role of  $A$  and  $B$  and repeat. For more details on the specific four-step Floquet-Langevin sequence see Appendix A.

*Discrete time crystal in a Floquet-Langevin simulation of the  $\pi$ -Toom model.*— Within the PCA setting, the  $\pi$ -Toom model is a discrete time crystal, and we have just described a procedure for “simulating” any PCA using continuous-time Floquet-Langevin dynamics. Naively, it seems that combining these two insights immediately yields a continuous-time, Floquet-Langevin DTC with an infinite lifetime. The subtlety is the following: at finite temperature, the errors due to Langevin noise (e.g., thermally activated escape out of the pinning potentials) may not satisfy the requirements of the Gács and Toom error models [Eq. (2)]. We will return to a detailed analysis of error correlations, but let us begin by numerically exploring the existence of time crystalline order in a Floquet-Langevin simulation of the  $\pi$ -Toom model.

Working with a two-dimensional square lattice, we perform an extensive set of numerical simulations by solving the Floquet-Langevin dynamics [Eq. (3)] using a symplectic stepping method. To implement the  $\pi$ -Toom model, we take the pinning potential to be  $V_{\text{pin}}(q) = v_{\text{pin}}(q-1)^2(q+1)^2 + Fq$ , where  $F = 10^{-4}$  breaks the



accidental Ising symmetry of the model. We parameterize the magnitude of the interaction and the pinning potentials as  $4v_I = v_{\text{pin}} = v$ , while the noise term,  $R_i(t)$ , is implemented via random momentum kicks with variance  $2\gamma T dt$ . Finally,  $\gamma$  is chosen such that the dynamics are tuned to critical damping relative to both  $V_{\text{pin}}$  and  $V_I$ .

In order to ensure that a single Floquet period implements only one  $\pi$ -Toom update, we utilize the following interleaving strategy: in step two, we choose  $\mathcal{T}$  to be the Toom update rule, while in step four, we choose  $\mathcal{T}$  to be the  $\pi$ -Toom update rule. We compute the Floquet-Langevin dynamics up to timescale,  $t \sim 10^4$ , starting from a uniform initial state (a study of different initial states is provided in the Supplemental Material [57]). We probe the resulting dynamics by measuring the average “magnetization,”  $\langle M_A \rangle \equiv (1/N) \sum_k \text{sign}(q_k^A)$ , where  $N = L \times L$  is the system size. Time crystalline order corresponds to stable period doubling of the magnetization; indeed, as shown in Fig. 1(d), the autocorrelation of the magnetization  $\langle M_A(t)M_A(0) \rangle$  exhibits period doubling out to a timescale that increases exponentially with  $L$  [57]. The DTC order parameter is then defined as the time average (over both space *and* time) of the stroboscopic magnetization:  $(-1)^{\lfloor t/\tau \rfloor} \langle M_A \rangle$ .

In order to compare our Floquet Langevin simulation with a direct implementation of the  $\pi$ -Toom PCA, we first translate the temperature,  $T$ , to an effective error rate  $P_E$  (per space-time unit cell) [91]. As shown in Fig. 1(a), the time crystalline order parameter, which we estimate from the time window  $t/\tau = 3000\text{--}3500$ , exhibits a phase transition as a function of  $P_E$ . The functional form and location of the DTC phase transition are in good agreement between our continuous-time Floquet Langevin simulation of the  $\pi$ -Toom model and a direct implementation of the PCA itself (with improving agreement for larger pinning potentials).

*The nature of errors in the Floquet-Langevin DTC.*— Because of the presence of a finite temperature bath, our continuous-time Floquet-Langevin simulation of the  $\pi$ -Toom model is intrinsically noisy. Large thermal fluctuations can lead to an “error” in the subsequent state  $\eta(\mathbf{x}, t)$  relative to the noiseless transition  $\mathcal{T}(\eta(\mathbf{x} + \mathcal{N}, t - 1))$ . Fortunately, our overall goal is in fact to simulate the noisy PCA version of the  $\pi$ -Toom model. However, even then, the distribution of errors arising from the Floquet-Langevin dynamics need not (*a priori*) be consistent with the aforementioned error condition [Eq. (2)].

To this end, our final goal is to obtain numerical evidence that: (i) the errors arising from the Floquet-Langevin dynamics satisfy Eq. (2) for some constant  $\epsilon(T)$  and (ii) the error bound  $\epsilon(T)$  can be made arbitrarily small as  $T \rightarrow 0$ . To begin, we first examine the temperature dependence of the error rate per space-time unit cell  $P_E = \langle E_u \rangle$ , where  $E_u = 0/1$  is the indicator function for an error at  $u$  [92]. In Fig. 2, we show the empirically measured error rate  $P_E(T)$  as a function of  $v/T$  for the Floquet-Langevin simulation of

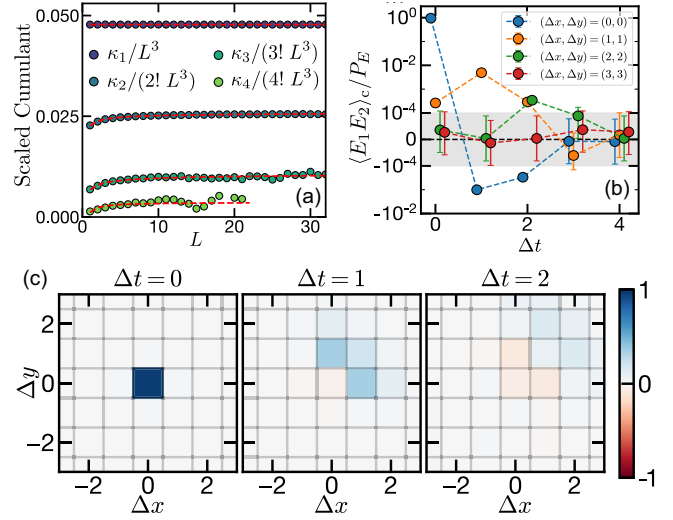


FIG. 3. (a) Scaled cumulants,  $\kappa_n/(L^3 n!)$ , of the error distribution from a Floquet Langevin simulation of the  $\pi$ -Toom model for  $L \times L \times L$  space-time volumes. The dashed curves are fits to  $\kappa_n/L^3 = c_n - b_n L^{-\mu_n}$ . As shown in the Supplemental Material [57], we find  $\mu > 0$  indicating convergence to a finite  $c_n$ . Each data point was estimated from the statistics of 3000 independent Langevin trajectories ( $T = 5.17$ ,  $v = 100$ ), with 1000  $L \times L \times L$  blocks sampled from each trajectory. (b),(c) The connected two-point correlations of the errors for  $v = 100$  and  $T = 5.17$ . The magnitude of the error correlations for a diagonal cut along space are depicted in (b), while the real-space propagation of errors is shown in (c). The color map range is rescaled by 1.0, 0.025, and 0.004 for the left, middle, and right panels, respectively.

three different PCA rules: the “do-nothing” rule  $\mathcal{I}$ , the Toom rule, and the  $\pi$ -Toom rule. In all cases we find that decreasing the temperature leads to an exponential decay in  $P_E$ , implying that for strong potentials and low temperatures, arbitrarily small error probabilities are obtained.

We now turn to the crucial issue of spatiotemporal correlations. Consider an arbitrary space-time volume  $V$  containing  $|V|$  points. Letting  $P(N_V)$  denote the probability that  $N_V$  errors occur in the volume  $V$ , we aim to provide empirical evidence that there is a constant  $\epsilon$  such that  $P(N_V = |V|) \leq \epsilon^{|V|}$  for all  $V$ . However, measuring  $P(N_V = |V|)$  directly is difficult because for large  $|V|$  such “large deviations” [93–96] are too rare to enable the collection of sufficient statistics. To make progress, we will instead relate  $P(N_V = |V|)$  to the connected  $n$ -point correlations of the errors. In particular, following the detailed derivations in Appendix B, our aim is to provide numerical evidence that the  $n$ th cumulant,  $\kappa_n$  does not grow faster than  $n!$  or  $|V|$ .

Restricting to space-time boxes of dimension  $|V| = L^3$ , we show the estimated cumulants for our Floquet-Langevin simulation of the  $\pi$ -Toom model for  $2 \leq L \leq 32$  [Fig. 3(a)]. They converge to a finite  $c_n$  with a power law correction in  $1/L$  [57]. While it is difficult to estimate the cumulants beyond  $n > 3$ , from the available data, the  $n!$  bound on  $c_n$  is safely satisfied. In addition to power-law correlations, the

nonzero higher-order cumulants also suggest that the error distribution is non-Gaussian. Interestingly, this originates from the anisotropic nature of the  $\pi$ -Toom update rule. An initial error causes an increased likelihood for errors at nearby space-time points, with correlations that propagate outward in the “NEC” direction [Figs. 3(b) and 3(c)].

In summary, despite errors which are both power-law correlated and non-Gaussian, we find compelling evidence that the Floquet-Langevin DTC satisfies the requisite error condition for absolute stability [52–56]. Of course we cannot rule out that for some anomalously large volume  $|V|$ , cumulant order  $n$ , or inverse temperature  $1/T$ , the observed behavior will change course and violate the bound—a caveat common to any numerical finite-scaling approach. Obtaining a rigorous proof of this bound thus remains an important open question.

*Note added.*—Recently, we became aware of complementary work exploring the utility of Toom-like dynamics for stabilizing time-crystalline phases in noisy, incoherent quantum spin systems [97].

We are greatly indebted to conversations with P. Gács for generously explaining various details of his work, C. Maes for pointing us to the literature on coupled map lattices, and C. Nayak and L. Balents for collaborations on related work. M. P. Z. is indebted to conversations with D. Huse during the initiation of this work. This work is supported in part by the Army Research Office (Grant No. W911NF2110262), the US Department of Energy, Office of Science, National Quantum Information Science Research Centers, Quantum Systems Accelerator (QSA), and the David and Lucile Packard Foundation. F. M. acknowledges support from the NSF through a grant for ITAMP at Harvard University.

*Appendix A: Details of the specific four-step Floquet-Langevin dynamics.*—We begin with the oscillators at site  $\mathbf{x}$  in the state  $(q_x^{A/B}, p_x^{A/B}) = (\eta(\mathbf{x}, t), 0)$ . From there, the dynamics evolve via a four-step process governed by [98]

$$H(t) = \sum_x \frac{(p_x^A)^2}{2m} + \frac{(p_x^B)^2}{2m} + U(t, \{q_x^A, q_x^B\}), \quad (\text{A1})$$

where the potential  $U(t, \{q_x^A, q_x^B\})$  has a Floquet period of  $\tau = 4$ :

$$U(t, \{q_x^A, q_x^B\}) = \begin{cases} \sum_x V_{\text{pin}}(q_x^A) + V_{\text{pin}}(q_x^B) & \text{mod}(\lfloor t \rfloor, 4) = 0, 2 \\ \sum_x V_{\text{pin}}(q_x^A) + V_I(q_{x+N}^A, q_x^B) & \text{mod}(\lfloor t \rfloor, 4) = 1 \\ \sum_x V_I(q_{x+N}^B, q_x^A) + V_{\text{pin}}(q_x^B) & \text{mod}(\lfloor t \rfloor, 4) = 3. \end{cases} \quad (\text{A2})$$

Let us unpack each of these steps in turn. First, we envision turning on a one-body potential,  $V_{\text{pin}}(q)$ , which has been engineered so that so that each  $q_x$  has local minima at  $q = \pm 1$ . At sufficiently low temperatures, the dissipative dynamics [Eq. (3)] will relax each oscillator’s positions,  $q_x$ , toward the nearest local minima, which corresponds to a valid state of the CA. The second step of the Floquet dynamics implements the cellular automaton transition  $B = \mathcal{T}(A)$ . We will keep  $q^A$  fixed using the pinning potential. For the  $B$  oscillators, however, we turn off  $V_{\text{pin}}$ , and turn on an interaction potential  $V_I$  between oscillators  $A$  and  $B$ . The interaction is engineered such that each oscillator  $B$  experiences a single potential minimum corresponding to the desired update rule as dictated by the oscillators  $A$  in its neighborhood; as a result,  $V_I$  depends on both  $q_x^B$  and  $q_{x+N}^A$ . In the third step, we turn off the interaction,  $V_I$ , while ramping up the pinning potential,  $V_{\text{pin}}$ . As in the first step, dissipation relaxes and pins the positions of the oscillators. Finally, in the last step, we implement “ $A = \mathcal{T}(B)$ ” by repeating step two with the role of  $A$  and  $B$  reversed [57]. Note that one can also replace the transition  $\mathcal{T}$  in the last step with the “do-nothing” CA rule,  $\mathcal{I}$ , if one wants to implement only a single CA update per Floquet cycle.

*Appendix B: Derivations relating  $P(N_V = |V|)$  to the connected  $n$ -point correlations of the errors.*—Consider the scaled cumulant generating function (SCGF),  $\lambda_V(j) = (1/|V|) \log \langle e^{jN_V} \rangle$ , which upper bounds the error probability as  $P(N_V = |V|) \leq e^{-|V|(j - \lambda_V(j))}$  for any choice of  $j \geq 0$ . The error bound from Eq. (2) can then be reexpressed via a min-max principle as

$$\ln(1/\epsilon) = \min_V \max_{j \geq 0} [j - \lambda_V(j)]. \quad (\text{B1})$$

Crucially, the Taylor series of the SCGF is directly related to the cumulants,  $\kappa_n$ , of the error distribution,  $\lambda_V(j) = |V|^{-1} \sum_{n=1}^{\infty} \kappa_n (j^n/n!)$ ; the cumulants themselves are in turn directly related to the connected correlations, e.g., for  $n = 2$ ,  $\kappa_2 = \sum_{u_1, u_2 \in V} \langle E_{u_1} E_{u_2} \rangle_c$ . If the correlations decay sufficiently rapidly as a function of distance, the cumulants will scale as  $\kappa_n \sim |V| c_n(V)$ , where the coefficient  $c_n(V)$  depends on the geometry of  $V$  but does not grow with  $|V|$  (i.e.,  $c_1(V) = P_E$ ). So long as this coefficient is upper bounded by some constant  $c_n \equiv \max_V c_n(V)$ , and  $c_n$  itself grows slower than  $n!$ , one can immediately upper bound  $\lambda_V(j) \leq \lambda(k) \equiv \sum_{n=1}^{\infty} c_n (k^n/n!)$  for all  $k \geq 0$ . It then follows that  $\ln(1/\epsilon) = \max_{j \geq 0} [j - \lambda(j)]$  also satisfies Eq. (2). Since  $\lambda(0) = 0$  and  $\lambda'(k) = P_E < 1$ , the maximal value is positive and finite, ensuring Eq. (2) is satisfied for some  $\epsilon < 1$ .

We now discuss whether the error bound  $\epsilon(T) \rightarrow 0$  as  $T \rightarrow 0$ , ensuring that by reducing the temperature of the

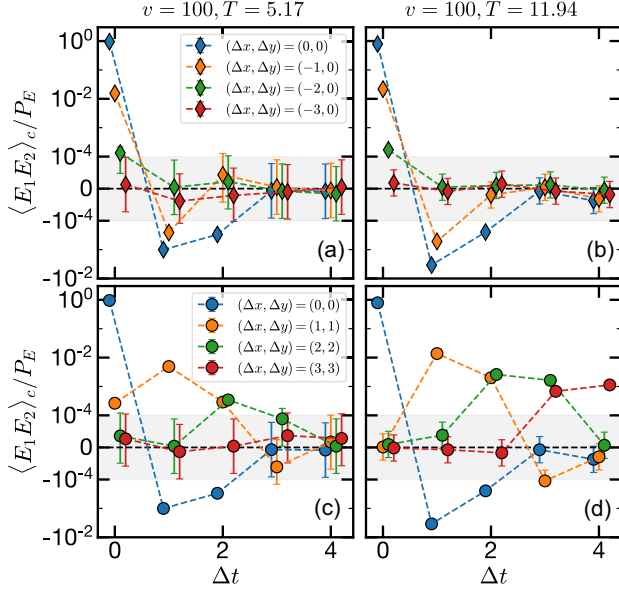


FIG. 4. Connected two-point correlations of the errors for  $v = 100$  and  $T = 5.17$  and  $T = 11.94$ . Along different directions, the errors display fundamentally distinct correlations, which are more prominent for higher temperature.

external bath, the error probability can be made arbitrarily small. One sufficient condition is the existence of a  $T$ -independent, continuous, and strictly increasing function  $\Lambda(k)$  such that  $\lambda(k) \leq P_E(T)\Lambda(k)$  for all  $k, T \geq 0$  and with  $\Lambda(0) = 0$ . To see why, note the aforementioned min-max principle now becomes

$$\log[1/\epsilon(T)] = \max_{j \geq 0} [j - P_E(T)\Lambda(j)]. \quad (\text{B2})$$

Since  $\Lambda(j)$  is invertible on  $j \in \mathbb{R}^+$ , we may define  $j_*(P_E) = \Lambda^{-1}(1/P_E)$ . Equation (B2) then provides the bound  $\log[1/\epsilon(T)] \geq j_*(P_E(T)) - 1$ . Finally, note  $\lim_{P_E \rightarrow 0} j_*(P_E) = \infty$ , because the inverse of a strictly increasing function is itself strictly increasing. Thus, the existence of such a  $\Lambda(j)$ , combined with our earlier evidence that  $\lim_{T \rightarrow 0} P_E(T) = 0$ , would imply  $\lim_{T \rightarrow 0} \epsilon(T) = 0$ .

To verify the existence of such a  $\Lambda(j)$ , it would be sufficient to show that the scaled cumulants are bounded as  $c_n(T) \leq P_E(T)C_n$ , with  $C_n$  growing slower than  $n!$ , so that  $\Lambda(j)$  has an infinite radius of convergence [Poisson

TABLE I. Fitting parameters for the power-law fit.

$n$	$T = 5.17, v = 100$ Fig. 3			$T = 11.94, v = 100$ Fig. S4		
	$c_n$	$b_n$	$\eta_n$	$c_n$	$b_n$	$\eta_n$
1	0.048	0	...	0.21	0	...
2	0.052	0.007	0.60	0.26	0.09	0.23
3	0.067	0.026	0.46	0.11	...	...
4	0.088	0.060	0.90	...	...	...

statistics corresponds to  $C_n = 1, \Lambda(k) = e^k$ ]. A preliminary comparison of  $T = 5.17, 11.94$  (Fig. 3 in the main text and Fig. 4 in the Supplemental Material [57]) finds  $c_2(T)/P_E(T) = 1.24$  at  $T = 11.94$ , while  $c_2(T)/P_E(T) = 1.08$  at  $T = 5.17$ , consistent with an approach to  $C_2 \sim 1$ , but a comprehensive investigation remains a work in progress (summary of the extracted cumulant fits can be found in Table I).

We end this appendix by complementing the data presented in Fig. 3(b) of the main text with additional space-time cuts as well as different temperatures [Fig. 4]. With regards to the space-time cuts, we observe that the correlations in errors are clearly anisotropic—when considering cuts in the negative  $\hat{x}$  direction (Fig. 4, top row), the correlations quickly become zero once the distance between the sites is greater than 2. On the other hand, when moving in the NEC direction, we find that error correlations are much greater and display a light-cone-like behavior—namely, errors a distance  $l$  away become meaningful after  $\Delta t = l$  steps have passed. This fact is further enhanced upon increasing the temperature of the system. When going from  $T \sim 5$  to  $T \sim 11$ , we observe that the correlated errors survive to much later times and spread to longer distances. These behaviors highlight the non-Markovianity of the noise in the Floquet-Langevin dynamics. Nevertheless, our present numerical results suggest that the noise satisfies the condition encoded in Eq. (2).

\*These authors contributed equally to this work.

- [1] A. C. Potter, T. Morimoto, and A. Vishwanath, Classification of interacting topological floquet phases in one dimension, *Phys. Rev. X* **6**, 041001 (2016).
- [2] V. Khemani, A. Lazarides, R. Moessner, and S. L. Sondhi, Phase structure of driven quantum systems, *Phys. Rev. Lett.* **116**, 250401 (2016).
- [3] D. V. Else, B. Bauer, and C. Nayak, Floquet time crystals, *Phys. Rev. Lett.* **117**, 090402 (2016).
- [4] N. Y. Yao, A. C. Potter, I.-D. Potirniche, and A. Vishwanath, Discrete time crystals: Rigidity, criticality, and realizations, *Phys. Rev. Lett.* **118**, 030401 (2017).
- [5] J. Zhang, P. Hess, A. Kyprianidis, P. Becker, A. Lee, J. Smith, G. Pagano, I.-D. Potirniche, A. C. Potter, A. Vishwanath *et al.*, Observation of a discrete time crystal, *Nature (London)* **543**, 217 (2017).
- [6] S. Choi, J. Choi, R. Landig, G. Kucsko, H. Zhou, J. Isoya, F. Jelezko, S. Onoda, H. Sumiya, V. Khemani *et al.*, Observation of discrete time-crystalline order in a disordered dipolar many-body system, *Nature (London)* **543**, 221 (2017).
- [7] D. V. Else, C. Monroe, C. Nayak, and N. Y. Yao, Discrete time crystals, *Annu. Rev. Condens. Matter Phys.* **11**, 467 (2020).
- [8] R. Nandkishore and D. A. Huse, Many-body localization and thermalization in quantum statistical mechanics, *Annu. Rev. Condens. Matter Phys.* **6**, 15 (2015).



- [9] P. Ponte, Z. Papić, F. Huveneers, and D. A. Abanin, Many-body localization in periodically driven systems, *Phys. Rev. Lett.* **114**, 140401 (2015).
- [10] D. A. Abanin, E. Altman, I. Bloch, and M. Serbyn, Colloquium: Many-body localization, thermalization, and entanglement, *Rev. Mod. Phys.* **91**, 021001 (2019).
- [11] J. A. Kjäll, J. H. Bardarson, and F. Pollmann, Many-body localization in a disordered quantum Ising chain, *Phys. Rev. Lett.* **113**, 107204 (2014).
- [12] M. Bukov, L. D'Alessio, and A. Polkovnikov, Universal high-frequency behavior of periodically driven systems: From dynamical stabilization to floquet engineering, *Adv. Phys.* **64**, 139 (2015).
- [13] D. A. Abanin, W. De Roeck, and F. Huveneers, Theory of many-body localization in periodically driven systems, *Ann. Phys. (Amsterdam)* **372**, 1 (2016).
- [14] S. A. Weidinger and M. Knap, Floquet prethermalization and regimes of heating in a periodically driven, interacting quantum system, *Sci. Rep.* **7**, 1 (2017).
- [15] D. A. Huse, R. Nandkishore, V. Oganesyan, A. Pal, and S. L. Sondhi, Localization-protected quantum order, *Phys. Rev. B* **88**, 014206 (2013).
- [16] A. Chandran, V. Khemani, C. R. Laumann, and S. L. Sondhi, Many-body localization and symmetry-protected topological order, *Phys. Rev. B* **89**, 144201 (2014).
- [17] Y. Bahri, R. Vosk, E. Altman, and A. Vishwanath, Localization and topology protected quantum coherence at the edge of hot matter, *Nat. Commun.* **6**, 7341 (2015).
- [18] I.-D. Potirniche, A. C. Potter, M. Schleier-Smith, A. Vishwanath, and N. Y. Yao, Floquet symmetry-protected topological phases in cold-atom systems, *Phys. Rev. Lett.* **119**, 123601 (2017).
- [19] D. A. Abanin, W. De Roeck, and F. Huveneers, Exponentially slow heating in periodically driven many-body systems, *Phys. Rev. Lett.* **115**, 256803 (2015).
- [20] D. V. Else, B. Bauer, and C. Nayak, Prethermal phases of matter protected by time-translation symmetry, *Phys. Rev. X* **7**, 011026 (2017).
- [21] T.-S. Zeng and D. N. Sheng, Prethermal time crystals in a one-dimensional periodically driven floquet system, *Phys. Rev. B* **96**, 094202 (2017).
- [22] T. Mori, Floquet prethermalization in periodically driven classical spin systems, *Phys. Rev. B* **98**, 104303 (2018).
- [23] F. Machado, G. D. Kahanamoku-Meyer, D. V. Else, C. Nayak, and N. Y. Yao, Exponentially slow heating in short and long-range interacting floquet systems, *Phys. Rev. Res.* **1**, 033202 (2019).
- [24] F. Machado, D. V. Else, G. D. Kahanamoku-Meyer, C. Nayak, and N. Y. Yao, Long-range prethermal phases of nonequilibrium matter, *Phys. Rev. X* **10**, 011043 (2020).
- [25] A. Kyprianidis, F. Machado, W. Morong, P. Becker, K. S. Collins, D. V. Else, L. Feng, P. W. Hess, C. Nayak, G. Pagano *et al.*, Observation of a prethermal discrete time crystal, *Science* **372**, 1192 (2021).
- [26] B. Ye, F. Machado, and N. Y. Yao, Floquet phases of matter via classical prethermalization, *Phys. Rev. Lett.* **127**, 140603 (2021).
- [27] A. Pizzi, A. Nunnenkamp, and J. Knolle, Classical prethermal phases of matter, *Phys. Rev. Lett.* **127**, 140602 (2021).
- [28] D. V. Else, W. W. Ho, and P. T. Dumitrescu, Long-lived interacting phases of matter protected by multiple time-translation symmetries in quasiperiodically driven systems, *Phys. Rev. X* **10**, 021032 (2020).
- [29] M. P. Zaletel, M. Lukin, C. Monroe, C. Nayak, F. Wilczek, and N. Y. Yao, Colloquium: Quantum and classical discrete time crystals, *Rev. Mod. Phys.* **95**, 031001 (2023).
- [30] K. Tucker, B. Zhu, R. J. Lewis-Swan, J. Marino, F. Jimenez, J. G. Restrepo, and A. M. Rey, Shattered time: Can a dissipative time crystal survive many-body correlations?, *New J. Phys.* **20**, 123003 (2018).
- [31] C. Lledó, T. K. Mavrogordatos, and M. H. Szymańska, Driven bose-hubbard dimer under nonlocal dissipation: A bistable time crystal, *Phys. Rev. B* **100**, 054303 (2019).
- [32] B. Buča and D. Jaksch, Dissipation induced nonstationarity in a quantum gas, *Phys. Rev. Lett.* **123**, 260401 (2019).
- [33] J. G. Cosme, J. Skulte, and L. Mathey, Time crystals in a shaken atom-cavity system, *Phys. Rev. A* **100**, 053615 (2019).
- [34] F. M. Gambetta, F. Carollo, A. Lazarides, I. Lesanovsky, and J. P. Garrahan, Classical stochastic discrete time crystals, *Phys. Rev. E* **100**, 060105(R) (2019).
- [35] F. M. Gambetta, F. Carollo, M. Marcuzzi, J. P. Garrahan, and I. Lesanovsky, Discrete time crystals in the absence of manifest symmetries or disorder in open quantum systems, *Phys. Rev. Lett.* **122**, 015701 (2019).
- [36] A. Lazarides, S. Roy, F. Piazza, and R. Moessner, Time crystallinity in dissipative Floquet systems, *Phys. Rev. Res.* **2**, 022002(R) (2020).
- [37] N. Dogra, M. Landini, K. Kroeger, L. Hruby, T. Donner, and T. Esslinger, Dissipation-induced structural instability and chiral dynamics in a quantum gas, *Science* **366**, 1496 (2019).
- [38] H. Keßler, J. G. Cosme, C. Georges, L. Mathey, and A. Hemmerich, From a continuous to a discrete time crystal in a dissipative atom-cavity system, *New J. Phys.* **22**, 085002 (2020).
- [39] H. Keßler, P. Kongkhambut, C. Georges, L. Mathey, J. G. Cosme, and A. Hemmerich, Observation of a dissipative time crystal, *Phys. Rev. Lett.* **127**, 043602 (2021).
- [40] H. Taheri, A. B. Matsko, L. Maleki, and K. Sacha, All-optical dissipative discrete time crystals, *Nat. Commun.* **13**, 848 (2022).
- [41] K. Kaneko, Period-doubling of kink-antikink patterns, quasiperiodicity in antiferro-like structures and spatial intermittency in coupled logistic lattice: Towards a prelude of a “field theory of chaos”, *Prog. Theor. Phys.* **72**, 480 (1984).
- [42] R. Kapral, Pattern formation in two-dimensional arrays of coupled, discrete-time oscillators, *Phys. Rev. A* **31**, 3868 (1985).
- [43] L. A. Bunimovich and Y. G. Sinai, Spacetime chaos in coupled map lattices, *Nonlinearity* **1**, 491 (1988).
- [44] K. Kaneko, Overview of coupled map lattices, *Chaos* **2**, 279 (1992).
- [45] K. Kaneko and T. Konishi, Transition, ergodicity and Lyapunov spectra of Hamiltonian dynamical systems, *J. Phys. Soc. Jpn.* **56**, 2993 (1987).
- [46] F. Wilczek, Quantum time crystals, *Phys. Rev. Lett.* **109**, 160401 (2012).

- [47] A. Shapere and F. Wilczek, Classical time crystals, *Phys. Rev. Lett.* **109**, 160402 (2012).
- [48] N. Y. Yao, C. Nayak, L. Balents, and M. P. Zaletel, Classical discrete time crystals, *Nat. Phys.* **16**, 438 (2020).
- [49] C. H. Bennett, G. Grinstein, Y. He, C. Jayaprakash, and D. Mukamel, Stability of temporally periodic states of classical many-body systems, *Phys. Rev. A* **41**, 1932 (1990).
- [50] J. Von Neumann, The general and logical theory of automata, in *Systems Research for Behavioral Science* (Routledge, New York, 1968), pp. 97–107.
- [51] S. Wolfram, Statistical mechanics of cellular automata, *Rev. Mod. Phys.* **55**, 601 (1983).
- [52] P. Gács, Reliable cellular automata with self-organization, *J. Stat. Phys.* **103**, 45 (2001).
- [53] L. F. Gray, A reader’s guide to gacs’s “positive rates” paper, *J. Stat. Phys.* **103**, 1 (2001).
- [54] A. L. Toom, Stable and attractive trajectories in multi-component systems, in *Advances in Probability* (Dekker, New York, 1980), Vol. 6, pp. 549–575.
- [55] C. H. Bennett and G. Grinstein, Role of irreversibility in stabilizing complex and nonergodic behavior in locally interacting discrete systems, *Phys. Rev. Lett.* **55**, 657 (1985).
- [56] D. Makowiec, Stationary states of Toom cellular automata in simulations, *Phys. Rev. E* **60**, 3787 (1999).
- [57] See Supplemental Material at <http://link.aps.org/supplemental/10.1103/PhysRevLett.131.180402> for additional details of the numerical simulations, the finite-scaling behavior of the time crystalline dynamics, and two experimental proposals, which includes Refs. [58–78].
- [58] J. Randall, C. Bradley, F. van der Gronden, A. Galicia, M. Abobeih, M. Markham, D. Twitchen, F. Machado, N. Yao, and T. Taminiau, Observation of a many-body-localized discrete time crystal with a programmable spin-based quantum simulator, [arXiv:2107.00736](https://arxiv.org/abs/2107.00736).
- [59] X. Mi, M. Ippoliti, C. Quintana, A. Greene, Z. Chen, J. Gross, F. Arute, K. Arya, J. Atalaya, R. Babbush *et al.*, Observation of time-crystalline eigenstate order on a quantum processor, [arXiv:2107.13571](https://arxiv.org/abs/2107.13571).
- [60] W. De Roeck and F. Huveneers, Stability and instability towards delocalization in many-body localization systems, *Phys. Rev. B* **95**, 155129 (2017).
- [61] P. J. Crowley and A. Chandran, Avalanche induced coexisting localized and thermal regions in disordered chains, *Phys. Rev. Res.* **2**, 033262 (2020).
- [62] J. I. Cirac and P. Zoller, Quantum computations with cold trapped ions, *Phys. Rev. Lett.* **74**, 4091 (1995).
- [63] T. H. Kim, P. F. Herskind, T. Kim, J. Kim, and I. L. Chuang, A surface electrode point Paul trap, *Phys. Rev. A* **82**, 043412 (2010).
- [64] P. Maunz, High optical access trap 2.0., Technical Report No. SAND–2016-0796R, 1237003, 618951, 2016.
- [65] J. Roßnagel, S. T. Dawkins, K. N. Tolazzi, O. Abah, E. Lutz, F. Schmidt-Kaler, and K. Singer, A single-atom heat engine, *Science* **352**, 325 (2016).
- [66] H.-K. Li, E. Urban, C. Noel, A. Chuang, Y. Xia, A. Ransford, B. Hemmerling, Y. Wang, T. Li, H. Haefner, and X. Zhang, Achieving translational symmetry in trapped cold ion rings, *Phys. Rev. Lett.* **118**, 053001 (2017).
- [67] S. Jain, J. Alonso, M. Grau, and J. P. Home, Scalable arrays of micro-penning traps for quantum computing and simulation, *Phys. Rev. X* **10**, 031027 (2020).
- [68] S. A. Moses *et al.*, A race track trapped-ion quantum processor, [arXiv:2305.03828](https://arxiv.org/abs/2305.03828).
- [69] U. Tanaka, M. Nakamura, K. Hayasaka, A. Bautista-Salvador, C. Ospelkaus, and T. E. Mehlstäubler, Creation of double-well potentials in a surface-electrode trap towards a nanofriction model emulator, *Quantum Sci. Technol.* **6**, 024010 (2021).
- [70] O. Katz, M. Cetina, and C. Monroe,  $N$ -body interactions between trapped ion qubits via spin-dependent squeezing, *Phys. Rev. Lett.* **129**, 063603 (2022).
- [71] O. Katz, L. Feng, A. Risinger, C. Monroe, and M. Cetina, Demonstration of three- and four-body interactions between trapped-ion spins, *Nat. Phys.* **1** (2023). [10.1038/s41567-023-02102-7](https://doi.org/10.1038/s41567-023-02102-7)
- [72] M. Brownnutt, M. Kumph, P. Rabl, and R. Blatt, Ion-trap measurements of electric-field noise near surfaces, *Rev. Mod. Phys.* **87**, 1419 (2015).
- [73] J. I. Costa-Filho, R. B. B. Lima, R. R. Paiva, P. M. Soares, W. A. M. Morgado, R. L. Franco, and D. O. Soares-Pinto, Enabling quantum non-markovian dynamics by injection of classical colored noise, *Phys. Rev. A* **95**, 052126 (2017).
- [74] T. P. Orlando, J. E. Mooij, L. Tian, C. H. van der Wal, L. S. Levitov, S. Lloyd, and J. J. Mazo, Superconducting persistent-current qubit, *Phys. Rev. B* **60**, 15398 (1999).
- [75] P. Krantz, M. Kjaergaard, F. Yan, T. P. Orlando, S. Gustavsson, and W. D. Oliver, A quantum engineer’s guide to superconducting qubits, *Appl. Phys. Rev.* **6**, 021318 (2019).
- [76] T. Menke, W. P. Banner, T. R. Bergamaschi, A. Di Paolo, A. Vepsäläinen, S. J. Weber, R. Winik, A. Melville, B. M. Niedzielski, D. Rosenberg, K. Serniak, M. E. Schwartz, J. L. Yoder, A. Aspuru-Guzik, S. Gustavsson, J. A. Grover, C. F. Hirjibehedin, A. J. Kerman, and W. D. Oliver, Demonstration of tunable three-body interactions between superconducting qubits, *Phys. Rev. Lett.* **129**, 220501 (2022).
- [77] C. M. Quintana *et al.*, Observation of classical-quantum crossover of  $1/f$  flux noise and its paramagnetic temperature dependence, *Phys. Rev. Lett.* **118**, 057702 (2017).
- [78] Y. Sung, F. Beaudoin, L. M. Norris, F. Yan, D. K. Kim, J. Y. Qiu, U. von Lüpke, J. L. Yoder, T. P. Orlando, S. Gustavsson *et al.*, Non-Gaussian noise spectroscopy with a superconducting qubit sensor, *Nat. Commun.* **10**, 1 (2019).
- [79] S. Ulam *et al.*, Random processes and transformations, in *Proceedings of the International Congress on Mathematics* (Citeseer, Cambridge, 1952), Vol. 2, pp. 264–275.
- [80] J. Neumann, A. W. Burks *et al.*, *Theory of Self-Reproducing Automata* (University of Illinois Press, Urbana, 1966), Vol. 1102024.
- [81] A. L. Toom, Nonergodic multidimensional system of automata, *Prob. Peredachi Inf.* **10**, 70 (1974).
- [82] D. Dawson, Stable states of probabilistic cellular automata, *Inf. Control* **34**, 93 (1977).
- [83] P. Gács, Reliable computation with cellular automata, *J. Comput. Syst. Sci.* **32**, 15 (1986).
- [84] Such behavior has also been referred to as asymptotic periodicity [85].
- [85] A. Lasota, T.-Y. Li, and J. Yorke, Asymptotic periodicity of the iterates of Markov operators, *Trans. Am. Math. Soc.* **286**, 751 (1984).



- [86] However, even for local interactions, Bennett *et al.* [49] argued long before the recent interest in time crystals that PCAs could give rise to stable subharmonic responses—a result we exploit here [34]. A particularly simple candidate for a PCA with time translation symmetry breaking is a majority-vote rule followed by a cyclic permutation [34]. However, as pointed out by Bennett *et al.* [49], this rule is not a stable time crystal for any period  $k > 2$ .
- [87] The origin of this stability can be intuitively understood as a form of error correction: The NEC majority vote eliminates any finite island of errors in a short time and as long as the error rate  $\epsilon$  is small enough, the system can eliminate an island before another equally large island appears [55,56,88].
- [88] P. Gacs, A new version of Toom’s proof, [arXiv:2105.05968](https://arxiv.org/abs/2105.05968).
- [89] G. Gielis and R. MacKay, Coupled map lattices with phase transition, *Nonlinearity* **13**, 867 (2000).
- [90] We note that the potential for the Toom rule to stabilize periodic behavior in PCAs was pointed out well before the recent interest in time-crystals [49,89].
- [91] For each temperature, we examine the ensemble of all simulated Langevin trajectories and count the number of errors under the continuous to discrete mapping  $S$ ; this allows us to empirically determine the error rate,  $P_E(T)$ .
- [92] We note that due to the spatiotemporal correlation of errors, the error rate is not the same as the error bound,  $P_E \neq \epsilon$ , but  $P_E$  will nevertheless play an important role in the analysis.
- [93] J.-D. Deuschel and D.W. Stroock, *Large Deviations* (American Mathematical Soc., Providence, 2001), Vol. 342.
- [94] S. S. Varadhan, *Large Deviations and Applications* (SIAM, Philadelphia, 1984).
- [95] F. Den Hollander, *Large Deviations* (American Mathematical Soc., Providence, 2008), Vol. 14.
- [96] H. Touchette, A basic introduction to large deviations: Theory, applications, simulations, [arXiv:1106.4146](https://arxiv.org/abs/1106.4146).
- [97] M. McGinley, S. Roy, and S. A. Parameswaran, Absolutely stable spatiotemporal order in noisy quantum systems, *Phys. Rev. Lett.* **129**, 090404 (2022).
- [98] Without loss of generality, we set the mass of the oscillator to be  $m = 1/2$  in the remaining discussions.